

SEDIMENTOLOGICAL STUDY OF DISTAL RAIN-TRIGGERED LAHARS: THE CASE OF WEST COAST OF ECUADOR

Maurizio Mulas¹, Kervin Chunga^{2,3}, Daniel Omar Garces Leon¹, Kenny Fernando Escobar Segovia¹

¹ Escuela Superior Politécnica del Litoral, ESPOL, Facultad de Ingeniería en Ciencias de la Tierra, Campus Gustavo Galindo Km 30.5 Vía Perimetral, P.O. Box 09-01-5863, Guayaquil, Ecuador. mmulas@espol.edu.ec; ogarces@espol.edu.ec; kescobar@espol.edu.ec

² Departamento de Construcciones Civiles Facultad de Ciencias Matemáticas, Físicas y Químicas Universidad Técnica de Manabí Avenue José María Urbina Portoviejo 130105, Ecuador. kchung@utm.edu.ec

³ Universidad Estatal Península de Santa Elena, UPSE, Facultad de Ciencias de la Ingeniería. Avda. Principal La Libertad, Ecuador.

ARTICLE INFO

Article history

Received August 10, 2018

Accepted March 12, 2019

Available online March 29, 2019

Handling Editor

Sebastian Richiano

Keywords

Ash deposits

Secondary lahar

Ecuador

Lithofacies

Risk

ABSTRACT

In this paper we present geological evidence of secondary rain triggered lahar that affected the central coast of Ecuador in the last 2ky. Eight main ash units were described in the field and then physically and petrographically characterized in the laboratory. The units present four main kinds of deposits testifying different depositional processes and the palaeotopographic condition of these sectors of Ecuador. The deposits recognized on the field are associable with granular flows with a high amount of water that compared with similar cases in the world not exceed run-out of 40km. The lateral variation inside the deposits recognized, considering the thickness and the distance from the main Holocene volcanoes (>160km), allows us to relate with secondary rain-triggered lahars and not with primary lahars. The presence of fine-grained ash of mm to the cm-thick layer above a cm to meter thick sand to gravel layer point out that these deposits are linked with single events and not with a continuous river sedimentation process. These events were triggered by rain that remobilized distal fallout deposits linked with the last 2ka eruptive activities of the Ecuadorian volcanoes as Quilotoa, Cotopaxi and Guagua Pichincha. Several units were identified in the deposits studied, and particularly it is possible to observe in one of them lateral variations of the deposits that permit to localize the debris flow body related to the secondary rain triggered lahar. The body of the debris flow is present in the coastal sector comprise between Crucita and Jama and it shows a lateral change in lithofacies related to different palaeo topographic conditions. In conclusion, in this paper, we show how the formation of secondary rain triggered lahar can occur in the coastal sector of Ecuador principally near the main river but also in flat topographic condition. Moreover, the presence of human bones and porcelain fragments also confirms that in the past, these events strongly affected old civilizations. Different municipalities as Manta, Bahia, San Vicente, Canoa, and Jama are undoubtedly exposed today to this kind of hazard. Further researches must be focused on the evaluations of the lahar volumes that can affect the coastal area of Ecuador.

INTRODUCTION

Lahar is the event of remobilization of loose

volcanic materials that can generate high-concentration sediment loaded flows, composed by sediments and water (Smith and Fritz, 1989; Smith and

Lowe, 1991; Pistolesi *et al.*, 2013). The lahar event may be triggered directly by the eruptive event (primary lahar) caused by failure of a crater lake (Massey *et al.*, 2010; Manville and Cronin, 2007) or “water” volcanic eruptions (Nairn *et al.*, 1979; Nemeth *et al.*, 2006; Kilgour *et al.*, 2010). This kind of geological event may be due to a remobilization of the volcanic material by heavy rain events even years after the eruption (secondary lahar - Rodolfo, 1989; Pierson *et al.*, 1992; Rodolfo *et al.*, 1996; Capra *et al.*, 2010; de Belizal *et al.*, 2013) but it can be triggered also without heavy rain events (Hodgson and Manville, 1999). The related deposits enclose the continuum between dilute stream flow (<20% sediment by volume) to hyperconcentrated flow (20-60% sediment by volume), passing to debris flow (>60% sediment by volume) and debris avalanche (Smith and Love, 1991; Doyle *et al.*, 2010). The related lithofacies testify a linear variation in sediment/water ratios, turbulence, grain dispersive forces, and fluid buoyancy. The term lithofacies is used to indicate a no-genetic and no-stratigraphic set of deposit features (grain size, sedimentary structures and local deposit geometries -Fisher and Schminke, 1984; Branney and Kokelaar, 2002), while “flow unit” is a depositional unit composed by single or multiple layers related with a single event, and in the field it can be identified by sharp contacts and by vertical changes in the lithofacies (Fisher and Schminke, 1984).

A rain-fall triggered lahar is a process that can occur by shallow landslides (Iverson and Lahusen, 1989; Crosta and Del Negro, 2003; Zanchetta *et al.*, 2004), rilling and erosion (Collins *et al.*, 1983) and rain splash erosion (Collins and Dune, 1988; Leavesley *et al.*, 1989; Manville *et al.*, 2000).

The coastal sector of Ecuador is poorly studied from the volcanological point of view. Previous studies (Usselman, 2010; Hall and Mothes, 2008; Mothes *et al.*, 1998; Hidalgo *et al.*, 2008) described fine ash layers, interbedded with clay and silt deposits, related to the Holocene eruptive activities of volcanoes like Cotopaxi (multiple eruptions that reach 4-5 VEI (Volcanic Eruption Index); Usselman, 2010), Quilotoa (800 BP -VEI 6; Mothes and Hall, 2008), Guagua Pichincha (VEI 4 eruptions; Hidalgo *et al.*, 2008) and Tungurahua (Hall *et al.*, 1999). Estrada *et al.* (1962) dated in 850 ± 105 yBP (years before present) one layer of Chirije area, strictly related to Manteña archeological horizon. Similar layers

were identified 50km southwestward to Manta by the mineral associations (Mothes and Hall, 2008). Archeological studies of Manteña civilizations (700-1500 AC - Harris *et al.*, 2004) have related these ash layers with the intense eruptive phases that affected Ecuador at 700-1100 years ago.

Large amounts of loose ash deposits on steep slopes, related with a periodical cycle of rains increase the chances that these deposits can be remobilized even several tens to hundreds of years after the eruption (*i.e.* Taupo - Smith 1991 and Pinatubo; Rodolfo *et al.*, 1996).

This work presents a sedimentological characterization of the volcanic ash layers cropping-out in the sector comprised between Salango and Jama (Fig. 1). The main goals are to explain what kind of events have generated these deposits and how these events affected this area. This study presents an unrecognized hazard for the coastal sector of Ecuador and that nowadays can affect the population of this sector, even if sited ~160km far from the nearest main eruptive centers.

LAST 5kyBP ERUPTIVE ACTIVITY OF ECUADOR

Ecuador is divided into three principal sectors N-S oriented: the coastal zone, Andes (central sector) and Orient (eastern sector) (Hall and Mothes, 2008). The central sector of Ecuador is part of the Northern volcanic zone (NVZ) of the Andes and it is a volcanic arc 650 km-long and 120 km wide, counting 84 volcanoes, 24 of these still active (Fig. 1). This sector is the result of the Nazca Plate subduction beneath the South American continental lithosphere (12 -22 My - Lonsdale, 1978) and it is divided into the Cordillera Occidental and Cordillera Real (Hall and Mothes, 2008).

In the last 5ky BP (before present), Ecuador was affected by multiple, high energetic eruptions (ranging from 4 and 6 VEI). Hall and Mothes (2008) recognized three main eruptive phases (4050 to 2090y BP, 2400 y BP and 980-810 y BP) related with the eruptive activities of the following volcanoes: Atacazo- Ninahuilca, Cayambe, Chimborazo, Cotopaxi, Guagua Pichincha, Pululahua, Quilotoa and Tungurahua (Table 1) (Papale and Rosi, 1993; Barberiet *et al.*, 1995; Samaniego *et al.*, 1998 and 2012; Robin *et al.*, 2008,2010; Hidalgo *et al.*, 2008; Mothes and Hall, 2008; Pistolesi *et al.*, 2011).

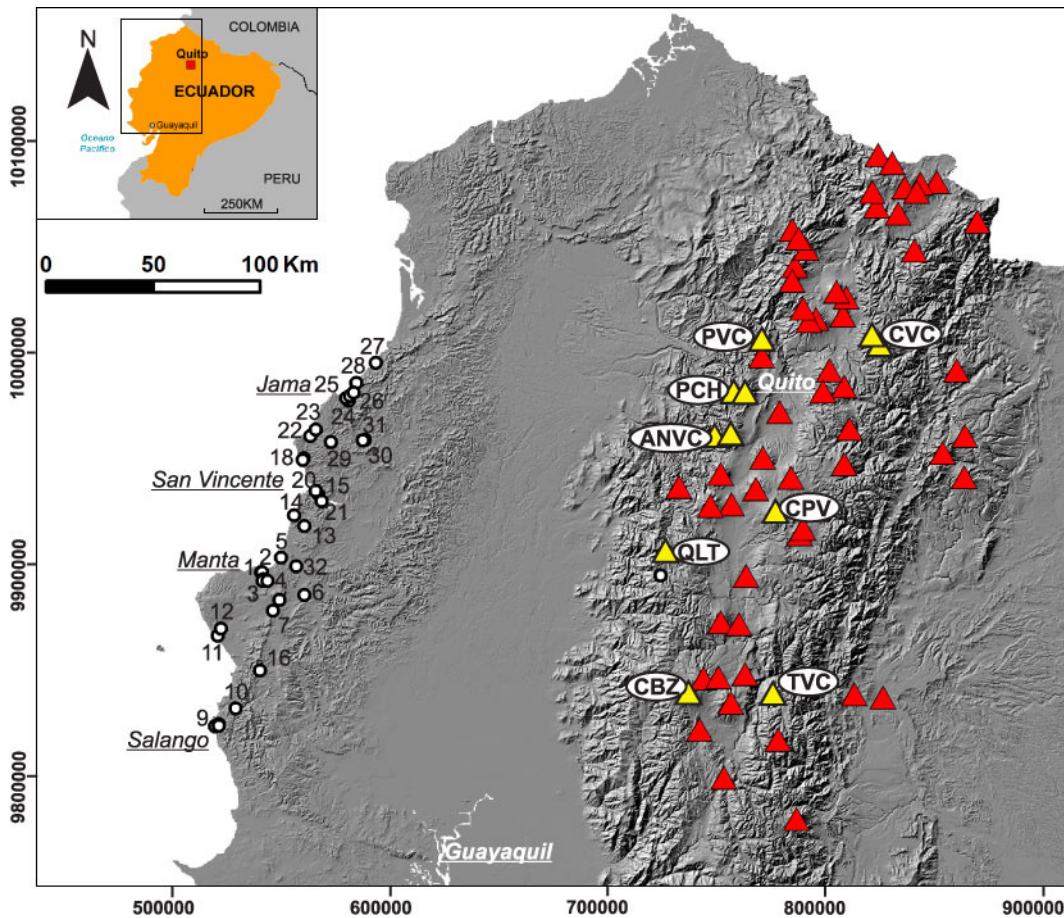


Figure 1. Stratigraphic sections (white dots) and the main volcanoes. Yellow triangles are the volcanic complex active in the last 5ky. CBZ: Chimborazo, TVC: Tungurahua, QLT: Quilotoa, CPV: Cotopaxi, ANVC: Atacazo-Ninahuilca, PCH: Pichincha, PVC: Pulahua and CVC: Cayambe.

The Pichincha Volcanic Complex (PCH), sited close to Quito, is composed by the older Rucu Pichincha edifice (active in the period comprise from 850 and 150 ky BP) and the younger Guagua Pichincha, active from 60ky BP to present. The eruptive history of Guagua Pichincha is divided into three main phases (Robin *et al.*, 2010): The Main Guagua Pichincha (60 to 11 ky BP), Toaza phase (9.8 to \approx 4 ky BP) and the Cristal Dome Phase (3.7 ky BP to present). During the Cristal Dome phase, characterized by dacitic tephra, the Guagua Pichincha volcano had four main eruptive cycles (Robin *et al.*, 2008). The first ones were comprised from 868 to 718 y BP; 2 ky BP a VEI 4 eruption occurred which cover the NW sector of Ecuador; 3 ky BP a VEI 5 eruption occurred that show an NW preferred ash dispersal direction (10-cm isopach sited 40km far from the vent). The last main eruptive phase of Guagua Pichincha was between 600 and 400 y BP and it was characterized by multiple VEI 4 eruptions with westward dispersion axes. The mineral assemblage of the Rucu Pichincha andesite

is composed mainly by plagioclase, orthopyroxene, and clinopyroxene with rare olivine and amphibole. The Guagua Pichincha products are more porphyritic constituted mainly by plagioclase with rare clinopyroxene and olivine (Samaniego *et al.*, 2010).

The Chimborazo volcano (CBZ), the highest of the NVZ with 6,268 m a.s.l., is sited 150 km southward from Quito in the Western Cordillera. The volcanic edifice has an elliptical shape base and it is composed of three main craters named Whymper, Politécnica and Martínez (Barba *et al.*, 2008). The eruptive history of Chimborazo is divided into four main phases (Samaniego *et al.*, 2012): Carihuarizo volcano (205-230 ky BP), Basal Edifice (CH-I; 120 - 60 ky BP), Intermediary edifice (CH-II; 48-35 ky BP) and Young cone (CH-III; 35ky BP to present). The eruptive activities during the CH-II phase were localized on Politécnica and Martínez peaks, while the CH-III activities were localized on Whymper peak. During the last eruptive phase, Chimborazo volcano produced andesitic surges, block and ash flows and scoria flows (Kilian *et al.*, 1995). The last

Volcano	Year of eruption	
Atacazo - Ninahuilca	BC4500-3990 (4), BC3270-2910 (5), BC400-230 (5)	(Hidalgo <i>et al.</i> 2008)
Cayambe	BC 1800, BC1650, BC1300, BC560, BC510, BC260, BC180, AD10, AD170, AD260, AD880, AD1040, AD1270, AD1570, AD1700, AD1785	(Samaniego <i>et al.</i> 1998)
Chimborazo	BC4130, BC2500, AD270, AD550	(Samaniego <i>et al.</i> 2012)
Cotopaxi	BC4350, BC3880, BC3280, BC2640, BC2050, BC1050, BC400, BC227, AD70, AD180, AD740, AD770, AD1130, AD1260, AD1350, AD1532-4, AD1742-44, AD1766, AD1877	(Barberi <i>et al.</i> 1995; Pistolesi <i>et al.</i> 2011, Hall and Mothes 2008)
Cuicocha	BC1150, BC950	(Hall <i>et al.</i> 1977)
Guagua Pichincha	BC1230, AD70, AD970, AD1660	(Robin <i>et al.</i> 2008)
Pululahua	BC690, BC450	(Papale and Rosi 1993)
Quilotoa	AD1150	(Mothes and Hall 2008)
Tungurahua	BC1010, AD730	(Hall <i>et al.</i> , 1999)

Table 1. Main eruptions that affected the coastal sector of Ecuador in the last 5ky.

Chimborazo eruptions occurred respectively in 6 ky BP, 4.5 ky BP, and during the 5th and 7th century (Barba *et al.*, 2008; Samaniego *et al.*, 2012). The products show a mineral assemblage constituted mainly by plagioclase and by rare free crystals of ortho and clinopyroxene, hornblende and oxide (Barba *et al.*, 2008).

The Cayambe Volcano Complex (CVC) is a composite volcano of 5,790 m high a.s.l. and it is sited 60 km NE from Quito. CVC is composed of three main edifices: Old Cayambe, Nevado Cayambe, and “Cono de la Virgen”. Six fall-out deposits, covering a large area of Ecuador, are linked with recent eruptive activities of Cayambe volcano (Hall and Mothes, 1994). Furthermore, the last 5kyBP was divided into three main eruptive phases (Samaniego *et al.*, 1998): Phase 1 (from 3.8 ky BP to 3.3kyBP), Phase 2 (2.5 ky BP to 2.2 ky BP) and Phase 3 (from 1.2 ky BP to the last eruption dated in 1785). The main eruptions of these three phases were generally VEI 4 eruptions. The mineral assemblages related to these eruptions are plagioclase, amphibole, clino- and orthopyroxene. Rare biotite is described in Cayambe products (Samaniego *et al.*, 2005).

The Cotopaxi volcano (CV– 5,897 m a.s.l.) is located in the eastern Cordillera, between the cities of

Latacunga and Quito. This volcano is characterized by a perfect cone shape with steep flanks (30°-35°) and a basal diameter of 22 km. It presents 3 main sectors with deep valleys: the northern Pita-Guayallambamba river system, the eastern Tambo-Tamboyacú river system and the western Barrancas and Saquimala river system (Pistolesi *et al.*, 2011). Cotopaxi is characterized by high frequency of explosive eruptions and high recurrence of lahar events. Moreover, due to the presence of a populated city in the proximity of the volcano make it one of the more dangerous volcanoes of Ecuador. The Cotopaxi volcano, during the last 5ky, has had an intense eruptive activity characterized by 19 eruptions classified as VEI>4 (Barberi *et al.*, 1995; Hall and Mothes, 2008) with column heights variable from 17 to 36 km (Pistolesi *et al.*, 2011) and a long series of lahar events that affected all the sector around the volcano (Mothes *et al.*, 2004; Pistolesi *et al.*, 2014). The deposits related with this phase are light grey, poorly sorted with a high percentage of black and grey obsidian fragments and red and grey banded rhyolite. The tephra chemical compositions vary from andesitic (56-62% SiO₂) to rhyolitic (70-75% SiO₂) (Hall and Mothes, 2008). The last eruptions of Cotopaxi appear quite regular by the mineralogical

point of view. The mineral assemblage includes plagioclase, clinopyroxene, orthopyroxene, and magnetite with rare olivine (Pistolesi *et al.*, 2011).

The Quilotoa Volcano (QLTV) is sited 75km SW from Quito and it shows a 2.8 km-diameter caldera that reaches a maximum elevation of 3,915 m a.s.l. on the south flank (Di Muro *et al.*, 2008). Starting from the Pleistocene, the Quilotoa volcano has had eight (8) eruptive cycles (named from the older one Q8 to Q2 - Hall and Mothes, 1992 and 2008) and the last one (Q1- 800 y BP) started after 14 ky of quiescence. The 800y BP Quilotoa eruption (VEI6) started with an early phreatomagmatic activity followed by a Plinian column phase that reached a maximum height of 35 km (Mothes and Hall, 2008). The following partial column collapse produced ash flows, surges and lag breccias. The final phase produced fine ash and ballistic block fall beds. The 800 y BP eruption of Quilotoa (mass discharge rate of $2 \times 10^8 \text{ kg s}^{-1}$) covered an area of $\sim 810,000 \text{ km}^2$. The surge and ash flow deposit volume were 2.5 km^3 and the total ash fall volume was 18 km^3 (Hall and Mothes, 2008; Mothes and Hall, 2008). The stratigraphic sequence of Q1 eruption consists of alternating m-thick levels of phreatomagmatic and Plinian block/lapilli fall deposits with surge, debris, and ash flow deposits. The ash falls events affected principally the eastern and north-eastern sectors, but the surge and lahar events affected all sectors around the volcano. The related fall deposits have white and light grey, vesiculated, crystal-rich ($\sim 48 \text{ wt}\%$) dacitic (65 wt% SiO_2) pumice lapilli and light grey rhyodacites lithic fragments (Rosi *et al.*, 2004). The white pumice present 24% of plagioclase, 12% of amphibole, 9% of biotite, 2% of oxides and sporadic quartz (Rosi *et al.*, 2004). This crystal assemblage is unique around Ecuador and it permits to easily recognize the Q1-Quilotoa eruption fall out deposits. After the 800 y BP eruption passed, the QLTV made a sequence of small eruptions and a series of limnic eruptions between 300 years BP and 220 y BP (Gunkel *et al.*, 2008).

The Tungurahua volcano complex (TVC) is a 5,023 m-high volcano sited on the Cordillera Real, characterized by steep slopes. Tungurahua volcano had three main eruptive phases divided by partial collapse cone events: Tungurahua I (33 ky BP to 14 ky BP), Tungurahua II (14 ky BP to 3 ky BP) and Tungurahua III (2.3ky BP to present) (Hall *et al.* 1999). The Tungurahua III is divided into two

periods named respectively Tungurahua III-1 (2.3 ky BP to 1.4 ky BP) and Tungurahua III-2 (1.4 ky BP to present). The deposits related with the last eruptive phase testify alternation of explosive and effusive activities (Hall *et al.*, 1999) with two main eruptions: one VEI 4 (1.3 ky BP) and one VEI 5 eruption (dated 1 ky BP). Plagioclase, augite, hypersthene, olivine and a trace of amphibole is the general mineralogical ensemble of Tungurahua volcano (Hall *et al.*, 1999).

The Pululahua volcanic complex (PVC), sited about 15km north from Quito, is a 3 x 2 km caldera with syn-caldera deposits and post-caldera dome deposits (Papale and Rosi, 1993). The eruptive history of PVC is divided into 4 main phases (Andrade and Molina, 2006): Phase I (old pre-caldera deposits), Phase II (young pre-caldera deposits), Phase III (syn-caldera deposits) and Phase IV (post-caldera deposits). The last main eruption occurred on 1.6 y BP. The complete stratigraphy of 2.2 ky BP eruption is divided into 10 units (named U1 to U10). The climax phase (U1), named Basal Plinian fall (Volentik *et al.*, 2010), developed in a nearly no-wind condition. The deposits are whitish, high vesiculated (from 72% to 80% voids), porphyritic (mineral assemblage with plagioclase, amphibole, and magnetite) pumice clasts and fresh to oxidized lithic lava fragments. The deposits related with a 32km height eruptive column (Pallini, 1996) are characterized by a high percentage of fine ash particles (75% wt. just at 6 km from the vent) and by a low free crystals percentage (Papale and Rosi, 1993).

For last, the Atacazo-Ninahuilca Volcanic complex (ANVC) is sited 10 km SW from Quito on the western cordillera. It is composed of La Carcacha, Atacazo and by several domes (Ninahuilca Chico I and II, la Cocha I and II and Arenal II) formed into the depression of the Atacazo edifice. From Pleistocene to Holocene, the ANVC volcanic complex made six eruptive phases and in the last 5ky BP made 2 large eruptions (named N5 and N6 - Hidalgo *et al.*, 2008). The N5 eruption (VEI5; 5.2 ky BP - 4.9 ky BP) produced fall out deposits covering the western sector of the volcanic complex. The deposits are characterized by yellow to orange pumice, grey and reddish hydrothermally altered dacitic lithics fragments, plagioclase and amphibole loose crystals staying into a coarse ash matrix. No biotite is described into the Atacazo products (Hidalgo *et al.*, 2008). The last ANVC eruption (N6 eruption-VEI 5) deposits have white to yellowish pumice, grey

to reddish hydrothermally altered lithic fragments, a loose crystal of plagioclase, amphibole and glass shards mixed into a coarse ash matrix (Hidalgo *et al.*, 2008). The deposits of this eruption were localized in the SW sector of the volcanic complex.

METHODOLOGY

To better characterize the ash deposits, 32 stratigraphical sections, sited in the area comprised between Salango and Jama (Manabí province - Ecuador) were described and laterally correlated. In this paper we present 8 main stratigraphical sections being these sections the more complete and resolute to explain the stratigraphical correlations. The stratigraphic correlation was made taking into account the physical and petrographic features of the deposits to recognize the marker layer. The main lithofacies were recognized on the base of sedimentological features change (texture and deposits geometry) and sedimentological structures.

The terminologies used in the deposit description are typically based on the direct observation of similar deposits and following characterization of volcanic deposits (Smith and Love, 1991; Fisher and Schminke, 1984; Branney and Kokelaar, 2002).

The main stratigraphic units were recognized by raw contacts, lithological features and by the presence of palaeosoils. Three samples (2 bulk palaeosols samples and one composed of charcoal fragments) were ¹⁴C-dated with the AMS methodology at the Beta Analytics Laboratories (Miami - USA). The grain-size analysis was made at ESPOL (Escuela Superior Politécnica del Litoral - Guayaquil) on dry samples into full steps of Φ ($-\log_{2}d$, with d : grain size in mm) between -6Φ and 8Φ . The principal statistical parameters were calculated according to Folk (1980) using the free software SFT (Tab. 2).

STRATIGRAPHY

The coastal sector of Ecuador is characterized by an irregular topography, recently tangled river networks and small catchment areas. The strong erosional processes that affected the studied area permit to observe the geometrical features of the deposits. This aspect will permit to understand the emplacement mechanisms and the palaeoenvironmental conditions. Ash layers were located within sand and clay sequence related to

coastal and fluvial environments. The deposits generally have thickness comprise between centimeter to meters and the contact between the ash layers and the other lithologies varied from sharp to mixed depending on the physical features of the single layers.

Unit A crops out only in Jaramijó area (Fig. 2). It is 20 cm thick and it presents at the base a sharp contact with the geological basement. Unit A is constituted by dark grey, medium- to fine-grained ash deposits with parallel stratification, micrometric rounded vesicles are visible into the matrix while free crystals and lithic fragments are absent. At the top, this unit is partially reworked showing an erosional contact with the above unit.

Unit B is well constrained into palaeo-topographic depressions (Fig. 2) with excellent outcrops at Jaramijó beach (sections 1 and 2 – Fig. 3a). It is divided into two subunits by a 3 cm thick sand layer and it shows high variability in thickness (from 0 to 61 cm thick in the Salango sector and from 0 to 140 cm in the Jaramijó area). Unit B is composed of whitish very fine-grained ash ($Md_{\Phi} = 4.10$), well to moderately sorted ($\sigma_{\Phi} = 0.72$) with parallel stratification. Rounded to sub-angular micro vesiculated whitish pumice with small Bt-crystals are present while free crystals and lithic fragments are rare ($<1\%$). Unit B outcrops at the base of a very complex stratigraphic sequence in the Río Chico area (section 9), near Salango where at the bottom (Fig.3c), it is 40 cm of thickness constituted by white, medium ash ($Md_{\Phi} = -0.28$), very poorly sorted ($\sigma_{\Phi} = 3.25$). Rarely lithics fragments (angular fragments of greenish claystone) and free crystals (plagioclase) are present. Porcelain and coal fragments related to human activities of Manteña civilization were found inside the matrix.

Unit C cropping out in section 1 and 2 (Jaramijó bay), presents an erosional contact at the base. It is composed of grey, massive, partially reworked medium to fine ash, poorly sorted matrix. The lithics fragments are greenish and reddish siltstone and claystone and also are presents archeological rests of Manteña civilization (porcelain and charcoal fragments). This unit is dated 1190 ± 30 y BP by ¹⁴C dating on charcoal fragments. In Río Chico (section 9) unit C is 5 cm thick and it is composed of light grey, massive, very fine ash ($Md_{\Phi} = 3.52$) with poorly sorted matrix ($\sigma_{\Phi} = 3.52$). In this sector, unit C appears strongly reworked with mixed contact at the

Samples	Bulk density	"F1 (<1mm)"	"F2 (< 1/16 mm)"	Median Diameter	Graphic Standard Deviation	Sorting	Graphic Kurtosis (KG)
	gr cm-3	%	%	Md-phi	Sigma-Phi		
PM-01	0.97	99.95	60.26	4.10	0.72	moderately sorted	0.98 mesokurtic
PM-02	0.99	99.62	65.11	4.20	0.68	moderately well sorted	1.05 mesokurtic
PM-04	1.34	78.00	21.88	2.65	3.18	very poorly sorted	1.19 leptokurtic
PM-05	0.86	12.19	5.08	-3.95	0.77	poorly sorted	2.94 very leptokurtic
PM-06	0.91	29.94	18.19	-4.05	4.43	very poorly sorted	0.56 very platykurtic
PM-07	0.89	89.66	52.81	3.95	1.33	very poorly sorted	1.91 very leptokurtic
PM-09	1.28	73.44	17.50	2.65	2.73	very poorly sorted	0.81 platykurtic
PM-10	1.27	82.12	19.14	3.20	2.40	very poorly sorted	1.60 very leptokurtic
PM-11	1.15	82.43	17.78	3.10	2.40	very poorly sorted	1.90 very leptokurtic
PM-13	0.91	41.16	18.13	-1.55	4.28	very poorly sorted	0.55 very platykurtic
PM-14	0.95	45.87	16.26	-0.55	3.80	very poorly sorted	0.62 very platykurtic
PM-15	1.07	23.20	5.31	-2.20	2.45	very poorly sorted	1.13 leptokurtic
PM-16	1.31	39.16	11.93	-2.15	3.93	very poorly sorted	0.64 very platykurtic
PM-17	1.04	53.57	18.06	0.30	3.70	very poorly sorted	0.63 very platykurtic
PM-18	1.24	68.26	8.04	2.10	3.30	very poorly sorted	0.70 platykurtic
PM-19	1.20	43.26	5.40	-0.95	3.33	very poorly sorted	0.69 platykurtic
PM-20	1.16	59.24	10.17	0.75	2.90	very poorly sorted	0.82 platykurtic
PM-21	1.10	87.76	51.13	3.95	1.95	poorly sorted	1.08 mesokurtic
PM-22	1.10	47.32	7.36	-0.35	3.43	very poorly sorted	0.67 very platykurtic
PM-23	1.25	43.69	21.05	-0.40	3.20	very poorly sorted	0.59 very platykurtic
PM-24	1.39	97.43	73.05	4.30	0.68	moderately sorted	2.00 very leptokurtic
PM-25	1.37	99.12	58.45	4.10	1.13	poorly sorted	1.10 mesokurtic
PM-26	1.07	96.19	68.21	4.20	0.90	poorly sorted	2.14 very leptokurtic
PM-27	1.17	72.54	25.44	2.15	2.68	very poorly sorted	0.72 platykurtic
PM-28	1.00	90.15	33.26	3.05	1.68	very poorly sorted	1.45 leptokurtic
PM-29	1.01	43.24	19.01	-3.40	4.40	very poorly sorted	0.50 very platykurtic
PM-30	1.04	99.45	69.83	4.25	0.73	moderately sorted	1.33 leptokurtic
PM-31	1.00	39.20	8.98	-1.20	3.30	very poorly sorted	0.70 platykurtic
PM-32	1.03	86.77	41.97	3.70	1.43	very poorly sorted	1.95 very leptokurtic
PM-33	1.04	87.53	44.11	3.75	1.50	very poorly sorted	1.85 very leptokurtic
PM-34	1.58	63.40	11.63	1.50	3.33	very poorly sorted	0.68 platykurtic
PM-35	1.37	56.67	9.82	0.80	3.58	very poorly sorted	0.67 platykurtic
PM-36	1.15	46.39	13.19	-0.10	3.02	very poorly sorted	0.61 very platykurtic
PM-39	0.96	99.12	64.34	4.07	0.82	moderately sorted	1.23 leptokurtic
PM-44	0.89	99.88	68.25	4.26	0.70	moderately sorted	1.21 leptokurtic
PM-45	1.00	96.23	65.26	4.10	0.95	poorly sorted	1.80 very leptokurtic
PM-46	0.92	95.26	50.97	3.77	1.33	poorly sorted	1.35 leptokurtic
PM-47	0.78	99.90	85.74	4.38	0.58	moderately well sorted	1.64 very leptokurtic
PM-48	1.02	98.95	48.50	3.90	0.80	moderately sorted	0.95 mesokurtic
PM-50	1.17	38.17	6.73	-0.70	2.60	very poorly sorted	0.80 platykurtic
PM-54	1.16	62.78	11.68	1.01	2.46	very poorly sorted	0.75 platykurtic
PM-55	1.14	38.57	11.00	-1.17	3.59	very poorly sorted	0.62 very platykurtic

Table 2. Main grain-size features of ash samples (F1: %<1mm; F2: % < 1/16 mm; Md_φ: Median Diameter; σ_φ: Graphic Standard Deviation and KG: graphic kurtosis).

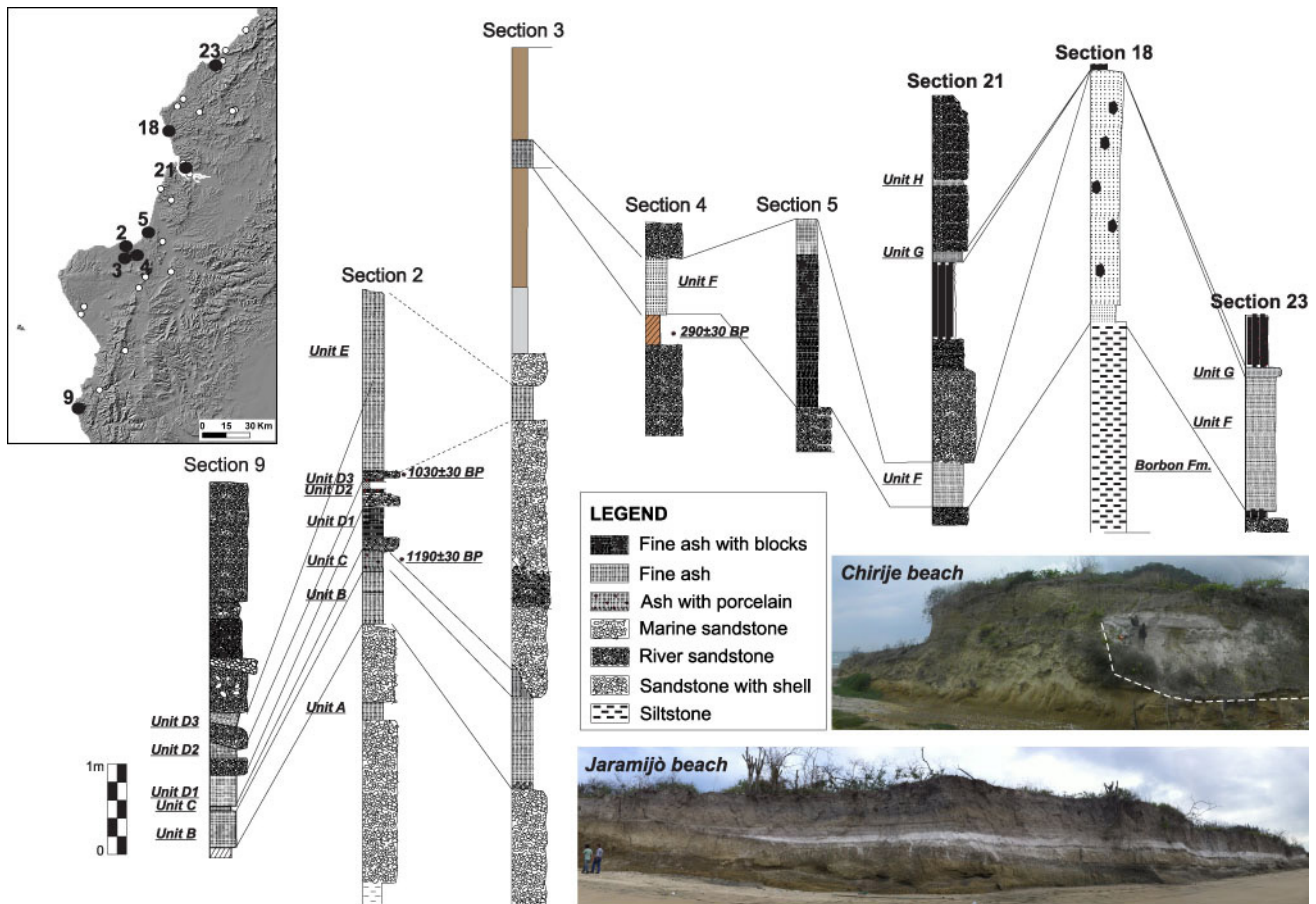


Figure 2. Lateral stratigraphic correlation of the coastal sector of Ecuador. The two photos are respectively Chirije and Jaramijó beach.

bottom and at the top.

The unit D is separate from the unit C by eroded contact and by an alternation of cm-thick sandy and clay layers. Unit D is composed by greyish, massive, medium to a fine ash with a poorly sorted matrix. Inside the matrix present a large amount of lithic fragments and mm-sized rounded vesicles (layer D1, D2, and D3 – Fig.3d). Into the ash deposits were found scour and fill structures, marine shells, porcelain fragment, food scraps and human bones (hands and arms) related to Manteña civilization (Usselman, 2010). Unit D is chronologically well constrained. The unit is dated 1030 ± 30 y BP (in this work) by the ^{14}C method on little charcoal fragments (burnt wood for cooking). The same unit in section 9 (Río Chico) is 34 cm thick. In this site, unit D is composed of a grey, massive fine ($Md_{\phi} = 0.70$) very poorly sorted ash ($\sigma_{\phi} = 2.81$). The matrix is characterized by the presence of mm-sized, rounded vesicles and white and grey pumice fragments. Three sub-layers, respectively 10 to 19 cm thick, 10 to 12 cm thick and

8 to 11 cm thick, were recognized into the sequence. The subunit shows the general features of Unit D but it presents a little sandy layer between the singles subunits.

Unit E is well exposed in sections 2 and 3 and it is 16 to ± 200 cm thick. It is composed of grey, massive fine ash. Inside the matrix, there is a high percentage of lithic rock fragments. Above the unit E, along the road from Manta to Crucita, was deposited a sandy layer, 1 meter thick, ^{14}C dated of 290 ± 30 y BP (this work). Unit E also outcrops at the bottom of the river sequence in “Estero Chirije Grande” near Chirije, and it presents a sharp contact at the bottom and a reworked contact at the top. This unit is composed of grey, fine ash ($Md_{\phi} = 3.52$) and poorly sorted matrix (leptokurtic with $\sigma_{\phi} = 1.80$). Mm-sized reddish lithics lava fragments ($< 5\%$) are presents into the matrix. This unit is separated by the latter ash unit by 428 cm thick of fine to medium sub-rounded sand and silt layer.

Unit F shows better expression of lateral variation

of all the units described. It is well exposed close to the water treatment basin, sited in the northern sector of San Vicente city (Fig. 1). This unit is composed by white, very fine ($Md_{\phi}=4.15$) ash matrix ($F1\%_{tot}<1\text{ mm} = 99\%$ and $F2\% <65\mu\text{m} = 64\%$) moderately sorted ($\sigma_{\phi}=0.85$) and with parallel stratification. Rarely mm-sized pumice fragments are present inside the matrix. This unit, at the bottom, presents a concordant sharp contact while at the top is irregular and locally reworked. In this sector, Unit F has a gradual lateral passage into a whitish, massive, medium ash with a poorly sorted matrix. Boulder-size lithic fragments and cm-sized pumice fragments are present. The larger boulders (30 cm) are grey, angular to sub-angular siltstones to claystones.

Unit F crops out also 2 km south-westward of Chone. It is 182 cm thick and it is composed of white, medium to fine ($Md_{\phi}= 3.47$), poorly sorted ($\sigma_{\phi} = 1.78$) ash layers with parallel stratification. At the top it presents, a white mm-thick very fine well-sorted ash, layer. Into the matrix, sub-angular siltstone lithic fragments (maximum size of 2 cm) and mm-sized rounded vesicles are observed. It presents sharp concordant contacts at the bottom and at the top.

Near Canoa city (section 18), Unit F is 245 cm thick. The first 15cm are composed by whitish, coarse ash ($Md_{\phi} = -0.30$), with a poorly sorted matrix ($\sigma_{\phi} = 3.10$). It is faintly stratified with mm-sized rounded vesicles. Sub-rounded pumice and greenish sub-rounded claystone fragments are present inside the matrix. The remnant 230cm are whitish, massive coarse ash ($Md_{\phi}=-0.80$) with a poorly sorted matrix (with $\sigma_{\phi} = 3.38$). Whitish micro-vesiculated, biotite-rich pumice lapilli (average size 3 cm) are well visible into the matrix. Sub-rounded to rounded claystones boulders have a maximum size of 50x37 cm and an average size of 10x10 cm.

Unit F in the Manta sector is 72cm thick and it is composed by a whitish, massive fine to medium ash with a poorly sorted matrix. Into the matrix are present whitish, cm sized, pumice fragments with sub-rounded vesicles. Lithic fragments are poor, and reddish porcelain fragments were found. The beneath soil is dated 290 ± 30 years BP by ^{14}C dating on total soil.

Moving northward to Crucita (section 5 – Fig.3b), Unit F shows strong lateral thickness variation (max. thickness 2.10m). The unit at the bottom is composed

of 60 cm thick whitish, massive, coarse ash ($Md_{\phi}=-1.11$) with very poorly sorted matrix ($\sigma_{\phi}=3.90$). It is faintly stratified, lapilli-rich, pumice poor and lithic-rich (<40%) unit with a no concordant sharp contact. Inside the matrix are present greenish and yellowish angular to sub-angular siltstone fragments. Gradually the unit coarsens upward, and it passes into a 50-cm thick level composed of a whitish, massive coarse ash to fine lapilli ($M_{\phi}=-1.93$) with a very poorly sorted matrix ($\sigma_{\phi}=3.55$). Into the matrix a large amount of greenish angular cm-sized (maximum size 12 cm) silt fragments are present. Upward the deposit is whitish, fine lapilli to coarse ash ($Md_{\phi} = -1.65$) with a very poorly sorted matrix ($\sigma_{\phi}=3.66$). Rounded microvesicles are present inside the massive matrix. The larger angular to sub-angular lithic blocks have a maximum size of 40 x 20 cm. Whitish, micro vesiculated crystal-rich (biotite and sanidine) cm-sized (average size 2 cm) pumice are present. The stratigraphic sequence of section 5 ends with 40 cm thick level and it is composed by whitish to brownish, fine rich ash layer with a poorly sorted ($\sigma_{\phi}=3.66$) coarse ash massive matrix. Mm-sized angular siltstone fragments and whitish sub-rounded cm-sized pumice are present into the matrix.

In Chirije beach (Fig.2), Unit F is strongly valley pounded into a palaeo-valley southward oriented and parallel respect to the beach line. It presents non-erosive contact where fine ash intruded the voids of the below deposit. The unit is composed of whitish fine rich ash layers ($Md_{\phi} = 3.47$) with poorly sorted matrix ($\sigma_{\phi} = 1.78$), generally with parallel stratification and separated by sharp contacts. Sporadic yellowish cm sized, angular fragments are present. Ripple structures of 4cm high and 15 cm large and water-pipes structures of 20 cm high are present into the unit.

Unit G in section 21 is 10 to 23 cm thick. It is composed of a light grey, very fine ash ($Md_{\phi} = 4.10$) with poorly sorted matrix ($\sigma_{\phi} = 0.95$). It is massive with a large percentage of lithic fragments. In the Jama area (section 28) the Unit G is composed of a grey, medium to fine ash ($Md_{\phi} = -0.78$) with very poorly sorted matrix ($\sigma_{\phi} = 2.60$). Whitish, mm-size rounded pumice and yellowish angular fragments of siltstones are presents into the matrix.

The last unit, Unit H, crops out only on the top of the San Vicente section (section 21 – Fig. 2) and it is 5 cm thick. It is composed by, light grey, rich in fine

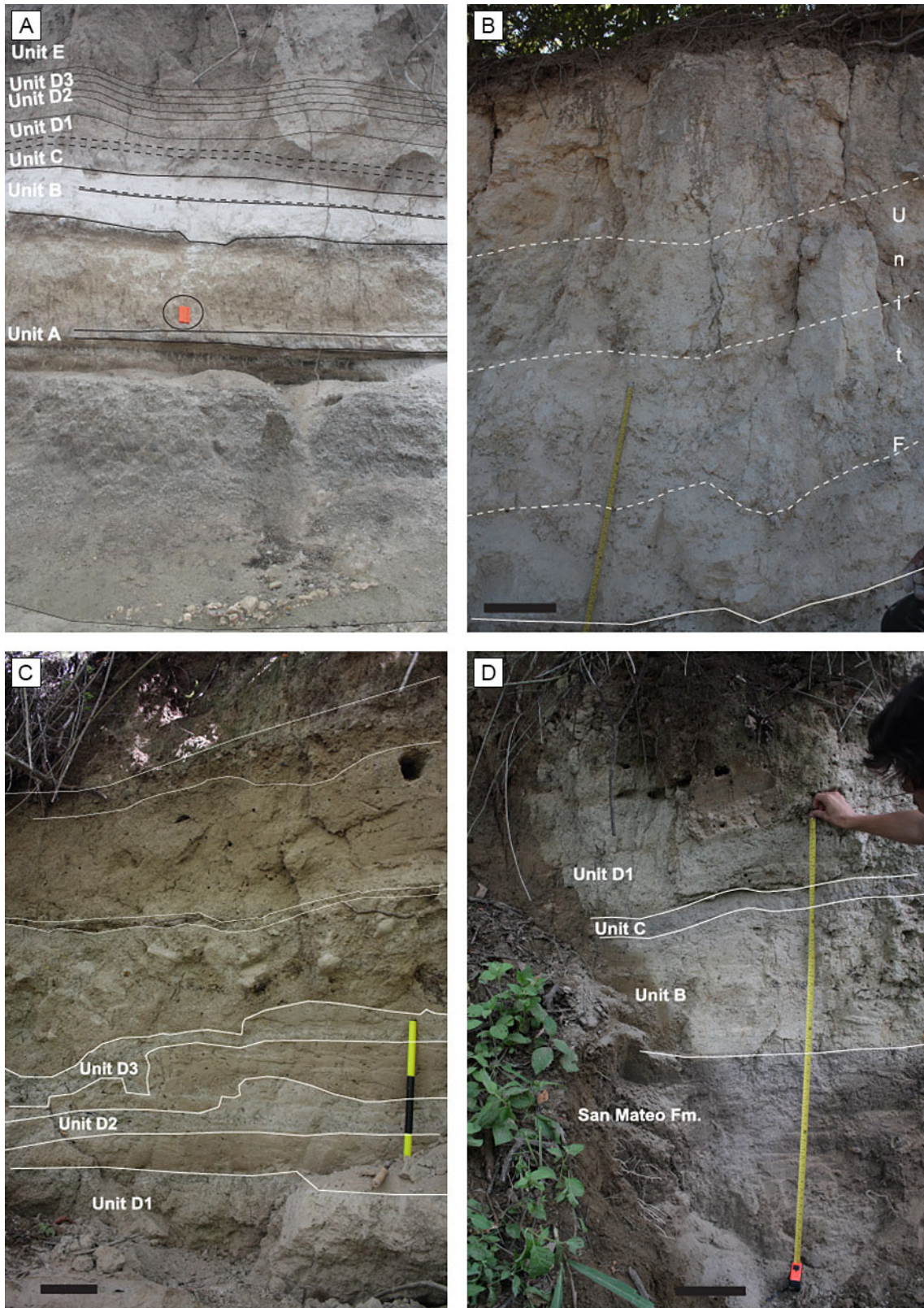


Figure 3. Detail of the studied outcrops: **a)** Section 2 “Jaramijó beach” where are well exposed the older ash units. Notebook for scale: 15 cm. **b)** Section 5 “Crucita” where are exposed strongly vertical lithofacies variations of unit F; **c)** Upper portion of section 9 sited in Río Chico where the ash layers are interbedded with sand layers by irregular contact; **d)** Lower portion of the section 9. In figures b), c) and d): scale bar: 20cm.

ash with the absence of lithic fragments and loose crystals, showing parallel stratification.

LAHAR DEPOSITS

Lithofacies of lahar deposits testify different type and magnitude of eruptions, climate conditions and topography conditions in the environments (Giordano *et al.*, 2002). In the studied area four main lithofacies were recognized and were named respectively F1, F2, F3, and F4.

The deposits of F1 crops-out on the coastal sector of Jaramijó (Unit A, B), in Chiriye (Unit F - near Bahía de Caraquez – Fig. 4a), San Vincenzo (Unit G, H) and near San Lorenzo. This type of deposit is cm to mm-thick, matrix-supported, finely parallel laminated to massive that fill the palaeo-valley. The matrix has mm-sized rounded micro-vesicles. The deposits with this lithofacies contain mm-sized, sub-rounded pumice and mm-sized angular to sub-angular lithic fragments (generally greenish sandstones and siltstones) set in very well sorted fine ash. It shows sharp contact at the bottom. Different structures as ripples, water-pipes (Fig.4b) and scour and fill structures (Fig. 4c) characterize this kind of deposit.

The deposit F2 (Fig. 4d) is very valley pounded, do not crops-out continuously along the sector and it was observed in Jaramijó (Unit D and Unit E), Crucita (Unit F - Fig.4e), Canoa (Unit F- Fig.4f), San Vicente (Unit F) and Jama (Unit F). The deposit is structureless and rarely matrix-supported. The clay content is less than 10 %. It consists of medium ash, m-thick, no-imbricated, very poorly sorted matrix with large (max. size 40 x 20 cm) angular to sub-rounded lithic blocks and mm- to cm-sized sub-rounded pumice. The last centimeters of the deposit at the top are faintly stratified coarse ash layer. This deposit shows sharp contacts at the bottom, while at the top is partially reworked. Laterally this deposit shows a gradual passage to the deposit F3.

The deposit F3 (Fig. 4j) is partially valley confined and locally it presents over banking evidence. It crops-out in Jaramijó (Unit C), San Vincente, Crucita (Unit F), Manta (Unit E) and Salango. The deposits consist of multiple (Fig. 4h), massive, poorly sorted fine ash layers. The top of the single “pulses” is mm-thick, compacted, micro-vesiculated very fine ash, (Fig. 4i). Contacts at the bottoms are generally sharp but locally can be irregular due to the superficial voids (Fig.4j).

The last type of deposit recognized in the field is the deposit F4. It crops out in Jaramijó (Unit D) and San Lorenzo (Unit D - Fig. 4g). It consists of faintly stratified, coarse-grained ash with poorly to very poorly sorted matrix. This deposit contains lithic and pumice clasts aligned which producing stratification. The deposits show sharp contacts both at the bottom and at the top.

DISCUSSIONS

The lahar events are the most frequent geological hazard associated with volcanic eruptions (Pistolesi *et al.*, 2013). According to the definition of lahar presented by Capra *et al.* (2004), we used the term lahar to indicate the origin of the flow related to remobilization of unconsolidated volcanic material. Large eruptions (VEI>3-4) characterized by large ash volume emissions during rainy periods (related with seasonal rain cycles or ENSO events), can generate hyperconcentrated flows and debris flows even months and years after the eruptions (Van Westen and Daag, 2005; Capra *et al.* 2010). The rain-triggered lahar can be also triggered at the beginning of rainy seasons with small rain amounts (Capra *et al.*, 2010). These events can be recognized in proximal vent sectors but also farther than 20 km from the source zone (De Belizal *et al.*, 2013). In the case of Ecuador, the ash deposits are present both in proximal vent sector as PDC (Pyroclastic Density Currents), primary lahars and fall-out deposits (Sierra sector) and in the coastal sector principally as fall-out deposits. Ash deposits related to lahar events in the area comprised between these two sectors were not previously described. The presence of large boulders inside the littoral sediments in the coastal deposits and the lack of volcanic deposits in this area comprise between the volcanic area and the coastal area support the idea that the deposits related with lahar event can be related principally with secondary remobilization processes triggered in the coastal sector.

Sedimentary processes and depositional environments

The different deposits recognized in the field testify erosional process, transport and deposition mechanism occurring during lahar events (Manville *et al.*, 2005) and a palaeo topographic setting

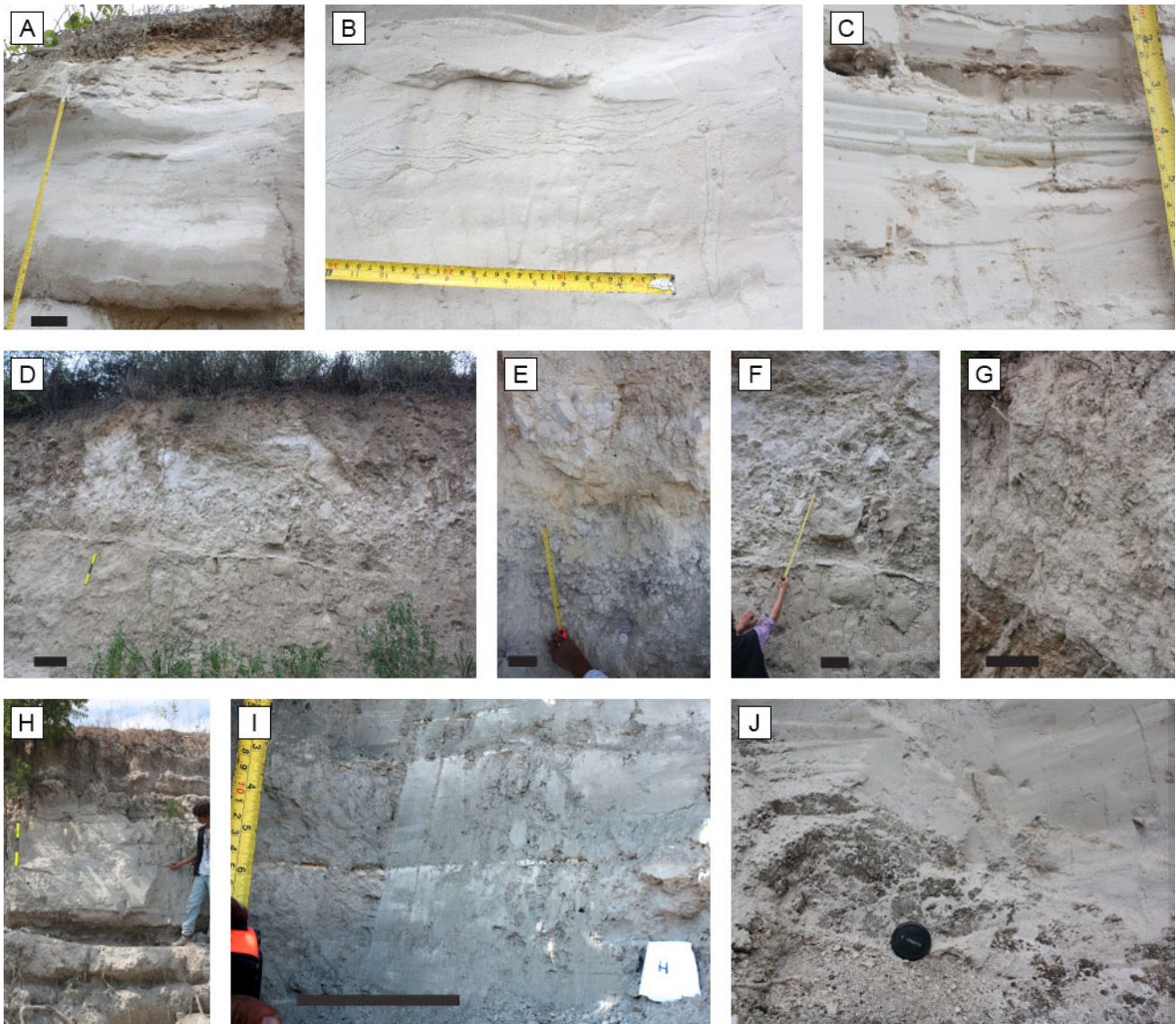


Figure 4. Details of the main lahars deposits outcropping in the west coast of Ecuador: **a)** The picture shows as the deposit F1 in Chirije is finely parallel laminated to massive filling a palaeovalley. Scale bar = 8 cm; **b)** Cm-sized ripples and water pipes structures present into the deposits F1 show testify a water saturated deposit; **c)** Scour and fill structures testifying reworking processes by water of the upper portion of the deposits in a shallow water environments; **d)** Valley pounded deposit F2 in Canoa characterized by the presence of metric sized boulders. Scale bar = 60 cm; **e)** Very poorly sorted matrix of the deposit F2 in Crucita with high percentage of boulders. Scale bar = 10 cm; **f)** Detail of meters sized sub rounded boulders into Deposit F2. Scale bar = 10 cm; **g)** Cm-sized lithic lapilli in faintly stratified deposit F4. Scale bar = 15 cm; **h)** Multiple massive poorly sorted fine ash layer of the meter thick deposit F3 in San Vicente. Person for scale = 170cm; **i)** Very fine compacted ash layers at the top of single layers in the deposit F3 in San Vicente. Scale bar = 8 cm; **j)** Fine ash intruded into surface irregularities in deposit F3 due to the presence of superficial voids: camera lens = 8.6 cm.

characterized by flat to a weakly engraved valley. Four main types of deposits were recognized and described.

In accordance with Smith and Lowe (1991) classification, the deposits cropping out along the coastal sector of Ecuador, varied from loose to weakly consolidated dilute stream flow to hyperconcentrated

flows to debris flows. According to this classification we consider the main structures present into the deposits (massive to faintly stratified) that permit to understand the flow features. The sorting and the presence or not of clay permit to understand the volcanic or not volcanic flow origin. Some structures allow to interpret if the flow is characterized by

turbulence or by laminar movements. Following the Scott (1995) classification, the deposits under study have features compatible with non-cohesive lahar to hyperconcentrated to water flows (Fig. 5).

In the deposit F1, we recognized scour and fill structures (in multiple, very well sorted layers present in Jaramijó area) that can be related to a shallow water environment (Schneider *et al.*, 2004). The ripple structures associated (Fig. 2b) with the scour and fill structures (Fig. 2c) are interpreted as a partial reworking of the upper part of the ash deposit due to a sediment-poor flow running over him in river environments. The presence of these structures allows interpreting this deposit as dilute streamflow, according to Smith and Lowe (1991) classification. The water pipes structures (Fig. 2b) associated with mm-sized roundish vesicles testify water saturated deposit during the first phases that ejected its water surplus due to a lithostatic pressure. The presence of sharp contacts and the thickness of the singles pulses permit to recognized single large volume events and not a continuum depositional process related for example with normal fluvial environments. The small average median diameter related with its sorting permit define these deposits as dilute streamflow to water flow deposits (Scott, 1995; Fig. 5) related to the front of the incoming flow or over banking flow. These conditions are characterized by a low sediment/water ratio that permits the moving of the flow both in flat topography and in a channelized river.

The deposit F2 shows absence of internal structures. This deposit is characterized by coarse-grained sediments, with low amount of clay and by a sub-rounded morphology of the boulders. This deposit is usually described into the “proximal” or “medial” (more or less 10km) facies in similar deposits (White Trachytic Tuff Cupa - Giordano *et al.*, 2002; Merapi volcano - de Belizal *et al.*, 2013; St. Helens - Smith and Lowe, 1991). These features testifying “*en-masse*” movements with strong grain-grain interactions. According to Smith and Lowe (1991), the low content of clay permits to interpret this kind of deposit as no-volcanic. It is important to mention that large boulder in no cohesive deposits cannot travel far. The coarser lahar deposits are usually localized only on a restricted area near deep slope gradients and they are characterized by small run-out. These features and the relative short run-out are interpreted as features of the flow body located

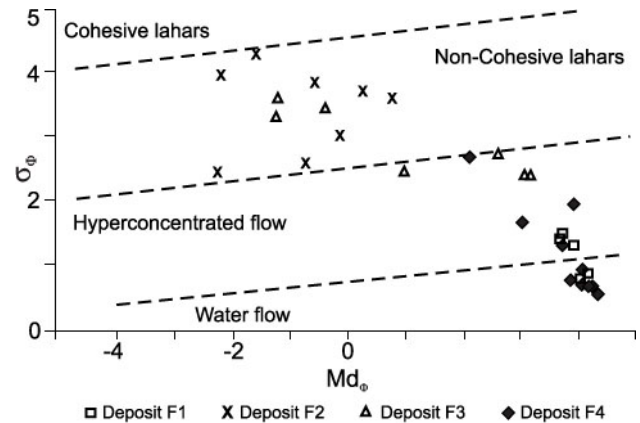


Figure 5. Distribution of the 4 facies (F1, F2, F3 and F4) identified in the lahar deposits analyzed in the coastal sector of Ecuador in accord with the Scott (1995) diagram for granular flow. The results show as the deposit F1 and F4 are comprised between water flow and hyperconcentrated flow. Deposit F2 shows the features of non-cohesive lahars and, at last, the deposit F3 shows features of non cohesive lahars and hyperconcentrated flow. (Md ϕ : Median Diameter; $\sigma\phi$: Graphic Standard Deviation).

near at the possible origin point. Deposits related to lahar events that traveled until 270 km from the vent (Cotopaxi 6 ky BP – Mothes and Wallace, 2015) show boulder percentage less than 5%. The strong hydrophobic features of ash layer made it possible to generate massive debris flows by sliding of the above layers. Time breaks into the depositional processes and the multiple pulses (large amount in short time) are testified by the very fine compacted ash layers present on the top of the single cm- to meters thick strata.

The deposit F2 passes gradually to deposit F3, which is massive to crudely stratified and clast-supported. The F3 deposit exhibits crude horizontal stratification. The faint stratification is evidenced by outsize cobble. These features strengthen the hypothesis that these deposits are related to non-cohesive hyperconcentrated flow. These features permit to interpret the deposit F3 as hyperconcentrated flow that has formed gradually by an original debris flow (deposit F2) during its run-out. The transformation from debris flow to hyperconcentrated flow is due to a dilution process when dry debris flow is mixing with a high amount of water related with snowmelt or heavy rainfall (Pierson and Scott, 1985). For these reasons, this deposit is not considered as primary lahar but better can be related with remobilization processes of ash

deposits (secondary lahars) that reach the coastal sector as fall ash and subsequently were removed by a high amount of water like heavy rain.

The absence of boulders compared to debris flows and the higher percentage of lapilli sized particles compared to the hyperconcentrated flow is interpreted as progressive settling out of the heavier fragments from the flow. These processes can be due to lower flow velocities into flatter topographical conditions and with the large run out regarding the massive unit. These kinds of deposits were described in Mount St. Helens (Pierson and Scott, 1985) and they were interpreted as a transformation from debris flow to hyperconcentrated flow at a distance comprised between 27 and 43 km (Capra *et al.*, 2010).

The deposit F4 is usually present at the bottom of F2 testifying a previous passage of the water richer flow head.

In general, all these deposits are interpreted generated by flows with a high sediment-water ratio.

Eight main ash units, related with the last 2ky Ecuadorian volcanic eruptions, were recognized in the coastal sector of Ecuador. On the base of mineralogical features (white pumice with biotite), bibliographic data of fall out ash dispersion directions (west-ward according with Mothes *et al.* 2008), and C¹⁴ dating allow as to conclude that Unit B can be related with remobilization of Quilotoa products. For the same reason unit F can be related to one of the 300-year BP Cotopaxi eruptions. The other units with similar mineralogical features can be interpreted as remobilization of the same source deposits at different times. Future studies are needed to confirm precisely the eruption generating the ash fall deposits present in the coastal sector that are remobilizing subsequently by rain events. All these units show similar features of rain triggered lahar described in other volcanoes (Merapi and Pinatubo – Rodolfo *et al.*, 1996; Capra *et al.*, 2010) but lesser than 40 km from the volcano. In the case of Ecuadorian coast, we observe deposits that don't show evidence of large run-out, but they are located at 160 km respect to the closer volcano (Quilotoa). The distribution of the deposits and the lithofacies recognized permit to interpret these deposits as generated by the landslide of fall out deposits from elevated topographies. The low amount of clay allows to interpret that these lahars are not related to a volcanic event but with gravity-driven process

forming by the failure of preexisting bedrock. The probable source of these lahars is near to the sites where deposits F2 are described (Salango, Canoa, and Jama).

CONCLUSIONS

On the coastal sector of Ecuador, eight main ash units were described and characterized and Unit B (from Salango to Jaramijó) and Unit F (from Jaramijó to Jama) show the greatest areal dispersions and the greater thickness. All these units are characterized by four main kinds of deposits testifying different depositional processes passing during secondary lahar events and the palaeo topographic condition of these sectors of Ecuador. These data permit to assert that different locations in the coastal sector of Ecuador in the last 2ky were affected by 8 main secondary lahars. The deposits recognized on the field are associable with granular flows that not exceed 40 km of run-out. The distance from the main Holocene volcanoes (>160km), deposits thickness and deposits features, allows us to say that are not primary lahars but are events of secondary lahars triggered by rain events. These events were triggered by remobilization of distal fallout deposits linked with the last 2ka eruptive activities of the Ecuadorian volcanoes and principally with Quilotoa and Cotopaxi eruptions. Unit F shows lateral variations in lithofacies that allow to localize the debris flow related to the secondary rain triggered lahar. The body of the debris flow is located in the sector comprise between Crucita and Jama showing a change in the features of the deposits related with different lateral palaeotopographic conditions (flat with shallow valley).

Some of the main localities of the coastal sector of Ecuador are localized near the valleys that show ash deposit. In the future, a similar process can recur and for this reason, the hazard related to secondary rain triggered lahars in the coastal area must be considered during the risk evaluation related to eruption processes. Different municipalities as Manta, Bahía, San Vicente, Canoa, and Jama are undoubtedly exposed today to this kind of hazard. Moreover, the presence of human bones and porcelain fragments also confirms that in the past, these events strongly affected old civilizations. In conclusion, this study shows evidence of secondary rain triggered lahar affecting the coastal sector of Ecuador and it

opens questions and further researches particularly focused on the evaluations of the lahar volumes that can affect the coastal area of Ecuador.

Acknowledgments

The authors are grateful to Rafael Alcivar and Cristina Lopez Coronel for the help during the fieldwork. This work was partially funded by the PROMETEO project of SENESCYT (Ecuador). We thank Sebastian Richiano, Ivan Petrinovic and Luis Lara for reviews and improve the quality of the manuscript.

REFERENCES

- Abràmoff, M.D., P.J., Magalhães and S.J., Ram, 2004. Image processing with Image. *Journal Biophotonics International*, 11:36-42.
- Andrade, D. and I. Molina, 2006. Pululahuá caldera: dacitic domes and explosive volcanism. In *Field guide for the COV4 meeting in Quito*.
- Barba, D., C., Robin, P., Samaniego and J.P. Eissen, 2008. Holocene recurrent explosive activity at Chimborazo volcano (Ecuador). *Journal of Volcanology and Geothermal Research* 176:27-35.
- Barberi, F., M. Coltelli, A. Frullani, M. Rosi and E. Almeida, 1995. Chronology and dispersal characteristics of recently (last 5ky) erupted tephra of Cotopaxi (Ecuador): implications for long-term eruptive forecasting. *Journal of Volcanology and Geothermal Research*, 69(3):217-239.
- Barberi, F., M. Coltelli, G. Ferrara, F. Innocenti, J.M. Navarro and R. Santacrose, 1988. Plio-Quaternary volcanism in Ecuador. *Geological Magazine* 125 (1):1-14.
- Branney, M.J. and B.P. Kokelaar, 2002. Pyroclastic density currents and the sedimentation of ignimbrites. *Geological Society of London*. 137 pp.
- Capra, L., L. Borselli, N. Varley, J.C. Gavilanes-Ruiz, G. Norini, D. Sarocchi, L. Caballero and A. Cortes, 2010. Rainfall-triggered lahars at Volcán de Colima, Mexico: Surface hydro-repellency as initiation process. *Journal of Volcanology and Geothermal Research*, 189 (1):105-117.
- Capra, L., M.A. Poblete and R. Alvarado, 2004. The 1997 and 2001 lahars of Popocatepetl volcano (Central Mexico): textural and sedimentological constraints on their origin and hazards. *Journal of Volcanology and Geothermal Research*, 131(3-4): 351-369.
- Chunga, K. and M.F. Quiñonez, 2013. Evidencia sedimentaria de tsunamis en la planicie aluvial de Villamil-Playas, Golfo de Guayaquil. *Acta Oceanográfica Del Pacífico*, 18 (1):163-180.
- Collins, B.D. and T. Dunne, 1988. Effects of forest land management on erosion and revegetation after the eruption of Mount St. Helens. *Earth Surface Processes and Landforms*, 13(3):193-205.
- Collins, B.D., T. Dunne and A.K. Lehre, 1983. Erosion of tephra-covered hill slopes north of Mount St. Helens, Washington: May 1980–May 1981. *Zeitschrift für Geomorphologische Naturwissenschaftliche Forschung*, 16(1):103-121.
- Crosta, G.B. and P. Dal Negro, 2003. Observations and modeling of soil slip-debris flow initiation processes in pyroclastic deposits: the Sarno 1998 event. *Natural Hazards and Earth System Science*, 3(1/2):53-69.
- De Bélizal, E., F. Lavigne, D.S. Hadmoko, J.P. Degeai, G.A. Dipayana, B.W. Mutaqin, M.A. Marfai, M. Coquet, B. Le Mauff, A.K. Robin and C. Vidal, 2013. Rain-triggered lahars following the 2010 eruption of Merapi volcano, Indonesia: A major risk. *Journal of Volcanology and Geothermal Research*, 261:330-347.
- Delannay, R., A. Valance, A. Mangeney, O. Roche, and P. Richard, 2017. Granular and particle-laden flows: from laboratory experiments to field observations. *Journal of Physics D: Applied Physics*, 50(5):1-40.
- Di Muro, A., M. Rosi, E. Aguilera, R. Barbieri, G. Massa, F. Mundula and F. Pieri, 2008. Transport and sedimentation dynamics of transitional explosive eruption columns: the example of the 800 BP Quilotoa Plinian eruption (Ecuador). *Journal of Volcanology and Geothermal Research*, 174(4):307-324.
- Doyle, E.E., S.J. Cronin, S.E. Cole and J.C. Thouret, 2010. The coalescence and organization of lahars at Semeru volcano, Indonesia. *Bulletin of Volcanology*, 72(8):961-970.
- Estrada, E., B.J. Meggers and C. Evans, 1962. Possible transpacific contact on the coast of Ecuador. *Science*, 135(3501):371-372.
- Fisher, R.V. and H.U. Schmincke, 2012. Pyroclastic rocks. Springer Science and Business Media. 471 pp.
- Folk, R.L., 1980. *Petrology of sedimentary rocks*. Hemphilliis, Austin. 182 pp.
- Giordano G., D. De Rita, M. Fabbri and S. Rodani, 2002. Facies associations of rain-generated versus crater lake-withdrawal lahar deposits from Quaternary volcanoes, central Italy. *Journal of Volcanology and Geothermal Research* 118:145-159.
- Gunkel, G., C. Beulker, B. Grupe and F. Viteri, 2008. Hazards of volcanic lakes: analysis of Lakes Quilotoa and Cuicocha, Ecuador. *Advances in Geosciences* 14:29-33.
- Hall, M.L. and P.A. Mothes, 2008. Quilotoa volcano - Ecuador: an overview of young dacitic volcanism in a lake-filled caldera. *Journal of Volcanology and Geothermal Research*. 176:44-55.
- Hall, M.L. and P.A. Mothes, 1994. Tefroestratigrafía Holocénica de los volcanes principales del Valle Interandino, Ecuador. El contexto geológico del espacio físico ecuatoriano. *Neotéctonica, geodinámica, volcanismo, cuencas sedimentarias, riesgo sísmico*, 6:47-68.
- Hall, M.L. and P.A. Mothes, 1992. Quilotoa Volcano-Ecuador. Eruption History and Possible Effects of Future Eruptions to the Hacienda San Juan, La Maná, Cotopaxi Province. Unpub. *Report for the Imperial Tobacco Company, Quito and London*.
- Hall, M.L., C. Robin, B. Beate, P.A. Mothes and M. Monzier, 1999. Tungurahua Volcano, Ecuador: structure, eruptive history and hazards. *Journal of Volcanology and Geothermal Research*, 91(1):1-21.
- Harris, M., V. Martínez, W.J. Kennedy, C. Roberts and J. Gammack-Clark, 2004. The Complex Interplay of Culture and Nature in Coastal South-Central Ecuador. *Expedition*, 46(1):38-43.
- Hidalgo, S., M. Monzier, E. Almeida, G. Chazot, J.P. Eissen, J. Van der Plicht and M.L. Hall, 2008. Late Pleistocene and Holocene activity of the Atacazo–Ninahuilca volcanic complex (Ecuador). *Journal of Volcanology and Geothermal Research*, 176(1):16-26.
- Hodgson, K.A. and V.R. Manville, 1999. Sedimentology and flow behavior of a rain-triggered lahar, Mangatoetoenui Stream,

- Ruapehu volcano, *New Zealand. Geological Society of America Bulletin*, 111(5):743-754.
- Iverson, R.M. and R.G. LaHusen**, 1989. Dynamic pore-pressure fluctuations in rapidly shearing granular materials. *Science*, 246(4931):796-799.
- Kilian, R., E. Hegner, S. Fortier and M. Satir**, 1995. Magma evolution within the accretionary mafic basement of Quaternary Chimborazo and associated volcanos (Western Ecuador). *Andean Geology*, 22(2):203-218.
- Knapp, G. and P.A. Mothes**, 1999. Quilotoa ash and human settlements. In: *Abya-Yala (Ed.). Actividad Volcanica y Pueblos Precolombinos en el Ecuador*, 139-156.
- Kilgour, G., V. Manville, F. Della Pasqua, A.G. Reyes, A.H. Graettinger, K.A. Hodgson and A.D. Jolly**, 2010. The 25 September 2007 eruption of Mt. Ruapehu, New Zealand: directed ballistics, Surtseyan jets, and ice-slurry lahars. *Journal of Volcanology and Geothermal Research* 191:1-14.
- Leavesley, G.H., G.C. Lusby and R.W. Lichty**, 1989. Infiltration and erosion characteristics of selected tephra deposits from the 1980 eruption of Mount St. Helens, Washington, USA. *Hydrological sciences journal*, 34(3):339-353.
- Lonsdale, P.**, 1978. Ecuadorian subduction system. *AAPG Bulletin*, 62(12): 2454-2477.
- Manville, V. and S.J. Cronin**, 2007. Breakout lahar from New Zealand's crater lake. *Eos, Transactions American Geophysical Union*, 88(43):441-442.
- Manville, V., K.A. Hodgson, B.F. Houghton and J.D.L. White**, 2000. Tephra, snow and water: complex sedimentary responses at an active snow-capped stratovolcano, Ruapehu, New Zealand. *Bulletin of Volcanology*, 62(4-5):278-293.
- Massey, C.I., V. Manville, G.H. Hancox, H.J. Keys, C. Lawrence and M. McSaveney**, 2010. Out-burst flood (lahar) triggered by retrogressive landsliding, 18 March 2007 at Mt Ruapehu, New Zealand—a successful early warning. *Landslides*, 7(3):303-315.
- Mothes, P.A. and M.L. Hall**, 1997. Quilotoa Caldera, Ecuador: a young eruptive centre in the western cordillera. *1997 IAVCEI General Assembly, Puerto Vallarta, Mexico*.
- Mothes, P.A. and M.L. Hall**, 2008. The plinian fallout associated with Quilotoa's 800 yr BP eruption, Ecuadorian Andes. *Journal of Volcanology and Geothermal Research*, 176:56-69.
- Mothes, P. A. and J.W. Vallance**, 2015. Lahars at Cotopaxi and Tungurahua Volcanoes, Ecuador: highlights from stratigraphy and observational records and related downstream hazards. In J. F. Shroder and P. Papale (Eds.) *Volcanic Hazards, Risks and Disasters*. Hazards and disasters series 1:141-168.
- Mothes, P.A., M.L. Hall and R.J. Janda**, 1998. The enormous Chillos Valley Lahar: an ash-flow-generated debris flow from Cotopaxi Volcano, Ecuador. *Bulletin of Volcanology*, 59(4):233-244.
- Mothes, P.A., M.L. Hall, D. Andrade, H. Yepes, T.C. Pierson, A. Gorki Ruiz and P. Samaniego**, 2004. Character, stratigraphy and magnitude of historical lahars of Cotopaxi volcano (Ecuador). *Acta vulcanologica*, 16(1/2):1000-1023.
- Mulas, M., R. Cioni and F. Mundula**, 2012. Stratigraphy of the Rheomorphic, Densely Welded, Monte Ulmus Ignimbrite (SW Sardinia, Italy). *Acta Vulcanologica*, 23(1/2):17-26.
- Nairn, I.A., C.P. Wood and C.A.Y. Hewson**, 1979. Phreatic eruptions of Ruapehu: April 1975. *Journal New Zealand Journal of Geology and Geophysics*. 22:155-173.
- Németh, K., S.J. Cronin, D. Charley, M. Harrison and E. Garae**, 2006. Exploding lakes in Vanuatu - 'Surtseyan-style' eruptions witnessed on Ambae Island. *Episodes* 29:87-92.
- Newhall, C. and R. Punongbayan**, 1996. Fire and mud: eruptions and lahars of Mount Pinatubo. *Philippine Institute of Volcanology and Seismology, Quezon City, and University of Washington Press (Seattle)* 1:989-1013.
- Pallini, R.**, 1996. Studio stratigrafico e granulometrico di un deposito di ricaduta da colonna pliniana in assenza di vento (Vulcano Pulumagua, Ecuador). *Università di Pisa, Pisa*. Phd thesys.
- Papale, P. and M. Rosi**, 1993. A case of no-wind plinian fallout at Pulumagua caldera (Ecuador): implications for models of clast dispersal. *Bulletin of Volcanology*, 55(7):523-535.
- Pierson, T.C. and K.M. Scott**, 1985. Debris Flow to Hyperconcentrated Streamflow. *Water resources research*, 21(10):1511-1524.
- Pierson, T.C., R.J. Janda, J.V. Umbal and A.S. Daag**, 1992. Immediate and long-term hazards from lahars and excess sedimentation in rivers draining Mt. Pinatubo, Philippines. U.S. Geological Survey *Water-Resources Investigations Report* 1:92-4039.
- Pistolesi, M., R. Cioni, M. Rosi and E. Aguilera**, 2014. Lahar hazard assessment in the southern drainage system of Cotopaxi volcano, Ecuador: Results from multiscale lahar simulations. *Geomorphology*, 207:51-63.
- Pistolesi, M., M. Rosi, R. Cioni, K.V. Cashman, A. Rossotti and E. Aguilera**, 2011. Physical volcanology of the post-twelfth-century activity at Cotopaxi volcano, Ecuador: Behavior of an andesitic central volcano. *Geological Society of America Bulletin*, 123(5-6):1193-1215.
- Pistolesi, M., R. Cioni, M. Rosi, K.V. Cashman, A. Rossotti and E. Aguilera**, 2013. Evidence for lahar-triggering mechanisms in complex stratigraphic sequences: the post-XII century eruptive activity of Cotopaxi Volcano, Ecuador. *Bulletin of Volcanology*. 75:698.
- Robin, C., P. Samaniego, J.L. Le Pennec, P.A. Mothes and J. Van Der Plicht**, 2008. Late Holocene phases of dome growth and Plinian activity at Guagua Pichincha volcano (Ecuador). *Journal of Volcanology and Geothermal Research*, 176(1):7-15.
- Robin, C., P. Samaniego, J.L. Le Pennec, M. Fornari, P.A. Mothes and J. Van Der Plicht**, 2010. New radiometric and petrological constraints on the evolution of the Pichincha volcanic complex (Ecuador). *Bulletin of volcanology*, 72(9): 1109-1129.
- Rodolfo, K.S.**, 1989. Origin and early evolution of lahar channel at Mabinit, Mayon Volcano, Philippines. *Geological Society of America Bulletin*, 101(3):414-426.
- Rodolfo, K.S., J.V. Umbal, R.A. Alonso, C.T. Remotigue, M.L. Paladio-Melosantos, J.H. Salvador, D. Evangelista and Y. Miller**, 1996. Two years of lahars on the western flank of Mount Pinatubo: Initiation, flow processes, deposits, and attendant geomorphic and hydraulic changes. *Fire and mud: eruptions and lahars of Mount Pinatubo, Philippines*, 1:989-1013.
- Rosi, M., P. Landi, M. Polacci, A. Di Muro and D. Zandomenighi**, 2004. Role of conduit shear on ascent of the crystal-rich magma feeding the 800-year-BP Plinian eruption of Quilotoa Volcano (Ecuador). *Bulletin of Volcanology*, 66(4):307-321.
- Samaniego, P., M. Monzier, C. Robin and M.L. Hall**, 1998. Late Holocene eruptive activity at Nevado Cayambe Volcano, Ecuador. *Bulletin of Volcanology*, 59(7):451-459.
- Samaniego, P., H. Martin, M. Monzier, C. Robin, M. Fornari, J.P. Eissen and J. Cotten**, 2005. Temporal evolution of magmatism in the Northern Volcanic Zone of the Andes: the geology and petrology of Cayambe Volcanic Complex (Ecuador). *Journal of*

petrology, 46(11):2225-2252.

- Samaniego, P., C. Robin, G. Chazot, E. Bourdon and J. Cotten**, 2010. Evolving metasomatic agent in the Northern Andean subduction zone, deduced from magma composition of the long-lived Pichincha volcanic complex (Ecuador). *Contributions to Mineralogy and Petrology*, 160(2), 239-260.
- Samaniego, P., D. Barba, C. Robin, M. Fornari and B. Bernard**, 2012. Eruptive history of Chimborazo volcano (Ecuador): A large, ice-capped and hazardous compound volcano in the Northern Andes. *Journal of Volcanology and Geothermal Research*, 221:33-51.
- Schneider, J.L., F.J.P. Torrado, D.G. Torrente, P. Wassmer, M.D.C.C. Santana and J.C. Carracedo**, 2004. Sedimentary signatures of the entrance of coarse-grained volcanoclastic flows into the sea: the example of the breccia units of the Las Palmas Detritic Formation (Mio-Pliocene, Gran Canaria, Eastern Atlantic, Spain). *Journal of volcanology and geothermal research*, 138(3):295-323.
- Smith, R.C.M.**, 1991. Landscape response to a major ignimbrite eruption: Taupo volcanic center, New Zealand. In: Fisher, R.V. and G.A. Smith, (Eds.), *Sedimentation in Volcanic Settings: SEPM, Special Publication, 45. Society for Sedimentary Geology, Tulsa, Oklahoma, USA*, 123-137.
- Smith, G.A. and W.J. Fritz**, 1989. Volcanic influences on terrestrial sedimentation. *Geology* 17:375-376.
- Smith, G.A. and D.R. Lowe**, 1991. Lahars: volcano-hydrologic events and deposition in the debris flow hyperconcentrated flow continuum. In: Fisher, R.V., Smith, G.A. (Eds.), *Sedimentation in Volcanic Settings: SEPM, Special Publication, 45. Society for Sedimentary Geology, Tulsa, Oklahoma, USA*, 59-70.
- Usselmann, P.**, 2010. Geodinámica y ocupación humana del litoral pacífico en el sur de Colombia y en el Ecuador desde el Holoceno (últimos 10 000 años). *Bulletin de l'Institut français d'études andines*, 39 (3):589-602.
- Van Westen, C.J. and A.S. Daag**, 2005. Analyzing the relation between rainfall characteristics and lahar activity at Mount Pinatubo, Philippines. *Earth Surface Processes and Landforms*, 30(13):1663-1674.
- Volentik, A.C., C. Bonadonna, C.B. Connor, L.J. Connor and M. Rosi**, 2010. Modeling tephra dispersal in absence of wind: insights from the climactic phase of the 2450 BP Plinian eruption of Pululagua volcano (Ecuador). *Journal of Volcanology and Geothermal Research*, 193(1):117-136.
- Whittaker, J.E.**, 1988. Benthic Cenozoic Foraminifera from Ecuador: Taxonomy and Distribution of Smaller Benthic Foraminifera from Coastal Ecuador (Late Oligocene-Late Pliocene). *British Museum of Natural History*.
- Zanchetta, G., R. Sulpizio, M.T. Pareschi, E.M. Leoni and R. Santacroce**, 2004. Characteristics of May 5-6, 1998 volcanoclastic debris flows in the Sarno area (Campania, southern Italy): relationships to structural damage and hazard zonation. *Journal of Volcanology and Geothermal Research*, 133(1):377-393.
- Zeidler, J.A. and D. Pearsall**, 1994. *Regional Archaeology in Northern Manabi, Ecuador*, Pittsburg/Quito: Univ. of Pittsburgh. *Memoirs in Latin American Archaeology*, 1.224 pp.